



**HAL**  
open science

## **Mechanical behaviour of a small-scale energy pile in saturated clay**

Neda Yavari, Anh Minh A.M. Tang, Jean-Michel Pereira, Ghazi Hassen

► **To cite this version:**

Neda Yavari, Anh Minh A.M. Tang, Jean-Michel Pereira, Ghazi Hassen. Mechanical behaviour of a small-scale energy pile in saturated clay. *Geotechnique*, 2016, 66 (11), pp.878 - 887. <10.1680/jgeot.15.T.026>. <hal-01515818>

**HAL Id: hal-01515818**

**<https://enpc.hal.science/hal-01515818v1>**

Submitted on 3 May 2017

**HAL** is a multi-disciplinary open access archive for the deposit and dissemination of scientific research documents, whether they are published or not. The documents may come from teaching and research institutions in France or abroad, or from public or private research centers.

L'archive ouverte pluridisciplinaire **HAL**, est destinée au dépôt et à la diffusion de documents scientifiques de niveau recherche, publiés ou non, émanant des établissements d'enseignement et de recherche français ou étrangers, des laboratoires publics ou privés.



HAL Authorization

# General Paper

## **Mechanical behaviour of a small-scale energy pile in saturated clay**

Neda YAVARI, Anh Minh TANG, Jean-Michel PEREIRA, Ghazi HASSEN

*Université Paris-Est, Laboratoire Navier (UMR CNRS 8205)*

### **Corresponding author:**

Dr. Anh Minh TANG

Université Paris-Est

Laboratoire Navier/Géotechnique (CERMES)

Ecole des Ponts ParisTech

6-8 avenue Blaise Pascal, Cité Descartes, Champs-sur-Marne

77455 Marne-la-Vallée

France

Email : [anhminh.tang@enpc.fr](mailto:anhminh.tang@enpc.fr)

Phone : +33 1 64 15 35 63

Fax : +33 1 64 15 35 62

25 **Abstract**

1  
2  
3 26 The mechanical behaviour of an energy pile in saturated clay under thermo-  
4  
5 27 mechanical loading was studied using a model pile. Axial load was first applied to the  
6  
7 28 pile head in steps to determine the resistance of the pile under mechanical load.  
8  
9  
10 29 Afterwards, thermo-mechanical tests were performed by applying a heating/cooling  
11  
12 30 cycle to the pile under constant axial load. The results show pile head heave during  
13  
14 31 heating and settlement during cooling. Irreversible settlement was observed after the  
15  
16  
17 32 thermal cycles. Tests performed with various axial loads show that the thermal  
18  
19 33 irreversible settlement is greater under a higher axial load.  
20  
21  
22

23 34

24 35 **Keywords:** energy pile; small-scale model; saturated clay; creep; thermo-mechanical  
25  
26  
27 36 load.  
28  
29

30 37

31  
32 38 Number of words: 4526  
33

34 39 Number of figures: 11  
35

36  
37 40 Number of tables: 0  
38  
39  
40  
41  
42  
43  
44  
45  
46  
47  
48  
49  
50  
51  
52  
53  
54  
55  
56  
57  
58  
59  
60  
61  
62  
63  
64  
65

41 **1. Introduction**

42 Energy piles are usually used in thermo-active foundations to transfer the mechanical load of  
43 the building to the ground and to provide heat exchange between the same using a ground-  
44 source heat pump system (Brandl, 2006; de Moel *et al.*, 2010; Brandl, 2013; Mimouni &  
45 Laloui, 2014; Olgun *et al.*, 2014). Full-scale tests on the thermo-mechanical behaviour of  
46 energy piles show that the temperature changes can modify stress and strain in the piles  
47 (Laloui *et al.*, 2003; Bourne-Webb *et al.*, 2009; Amatya *et al.*, 2012; McCartney & Murphy,  
48 2012; Murphy *et al.*, 2014; Wang *et al.*, 2014). Reduced-scale tests on energy piles in sand  
49 show sometimes contradictory trends: their shaft resistance decreased in capacity after  
50 thermal loading was introduced, after Wang *et al.* (2011), while Ng *et al.* (2015) found an  
51 increase of shaft resistance after heating. Stewart & McCartney (2013) found that the  
52 behaviour of a scale-model energy foundation tested in a geotechnical centrifuge during  
53 transient heating and cooling, agrees well with observation on full-scale end-bearing energy  
54 foundations reported in the literature. Numerical simulations reveal that the effect of  
55 temperature on the mechanical behaviour of the piles is mainly related to its thermal  
56 expansion/contraction (Laloui *et al.*, 2006; Péron *et al.*, 2011; Yavari *et al.*, 2014a).

57  
58 However, it is well known that temperature might slightly modify the mechanical properties  
59 of saturated clay (Cekerevac & Laloui, 2004; Hueckel *et al.*, 2011; Hong *et al.*, 2013; Laloui *et*  
60 *al.*, 2014). In addition, irreversible volume change of soil induced by temperature variations  
61 (i.e. contraction of normally consolidated clay during heating, see Abuel-Naga *et al.* 2007)  
62 may have significant effects on the undrained shear strength of the soil, which may affect  
63 the foundation capacity during rapid loading. Also, heating could induce a small decrease of  
64 the shear strength of clay/concrete interface (Di Donna & Laloui, 2013; Murphy &

1  
2  
3  
4  
5  
6  
7  
8  
9  
10  
11  
12  
13  
14  
15  
16  
17  
18  
19  
20  
21  
22  
23  
24  
25  
26  
27  
28  
29  
30  
31  
32  
33  
34  
35  
36  
37  
38  
39  
40  
41  
42  
43  
44  
45  
46  
47  
48  
49  
50  
51  
52  
53  
54  
55  
56  
57  
58  
59  
60  
61  
62  
63  
64  
65  
66  
67  
68  
69  
70  
71  
72  
73  
74  
75  
76  
77  
78  
79  
80  
81  
82  
83  
84  
85  
86  
87  
88

McCartney, 2014). As a result, beside the thermal expansion/contraction of the piles, other phenomena should be considered as well when studying the mechanical behaviour of energy piles in clay. Conducting full-scale tension load tests, Akrouch *et al.* (2014) found that heating increases the creep rate of energy piles in high plasticity clay.

Beside direct effects of temperature changes, the impact of cyclic heating/cooling on energy piles has been studied in various works. Ng *et al.* (2014) performed centrifuge modelling of energy piles subjected to heating/cooling cycles in saturated clay under constant working load and observed cumulating irreversible displacement (thermo-mechanical ratcheting) over five thermal cycles. This irreversible settlement reached 3.8% of pile diameter in lightly overconsolidated clay and 2.1% of pile diameter in heavily overconsolidated clay. Yavari *et al.* (2014b) found that a heating/cooling cycle applied on a model pile inserted in dry sand under constant axial load induced an irreversible displacement of around 2% of the pile diameter. Amatya *et al.* (2012) analysed the results of several in situ experiments on energy piles and concluded that heating/cooling cycles induce volume change of the energy piles, which changes the pile-soil interaction. More precisely, the mobilized shaft resistance profile of a mechanically loaded pile may undergo significant changes during thermal loading. After Ng *et al.* (2014), beside the mobilisation of shaft resistance, thermo-mechanical ratcheting can be attributed to a cumulating irreversible reduction of confining stress at the pile-soil interface.

In the present work, the mechanical behaviour of energy piles in saturated clay is investigated using a small-scale model. Heating/cooling cycles were performed under various constant axial loads. The pile head axial displacement was monitored during these thermo-mechanical loads.

## 89 2. Experimental method

90 The experimental setup is presented in Figure 1. This system is similar to that used in Yavari  
91 *et al.* (2014b). A pile was embedded in a container filled with saturated clay. The model pile  
92 was a closed-end aluminium tube with outer and inner diameters of 20 and 18 mm,  
93 respectively. The total length of the pile was 800 mm but only 600 mm was embedded in  
94 soil. The pile was coated with a layer of Fontainebleau sand (median grain size of 0.23 mm)  
95 by means of appropriate glue (Araldite). The added roughness will likely force failure to  
96 occur in the clay, which is softer, rather than at the interface.

97 The axial load applied to the pile head was controlled by the water level in the tank. A force  
98 sensor placed on the pile head measured pile head axial load. A displacement sensor  
99 monitored the pile head settlement. A heating/cooling circulating bath (cryostat) allowed  
100 the control of the pile temperature. Its internal reservoir was filled with water and  
101 connected to an aluminium U-shaped tube (2 mm internal diameter) inside the pile. The pile  
102 was filled with water to ensure the thermal transfer between the U-shaped tube and the  
103 pile. One temperature sensor was inserted inside the pile to monitor its temperature during  
104 the experiments. Note that the pile temperature will not be homogenous but it may be an  
105 appropriate assumption for the nature of the analysis in the present study.

106 Kaolin clay was used in this study. Its particle size distribution, obtained by laser diffraction  
107 method, is shown in Figure 2. It has a liquid limit of 57%, a plastic limit of 33%, and a particle  
108 density of 2.60 Mg/m<sup>3</sup>. More details about this material can be found in the work of  
109 Muhammed (2015). The soil powder was mixed with distilled water to a water content of  
110 29% and then stored in hermetically sealed boxes for more than 24 h to ensure moisture  
111 homogenisation. Soil compaction started with three layers of 100, 100 and 50 mm. A

112 vibratory hammer was used to compact the soil to a dry density of  $1.45 \text{ Mg/m}^3$  (that  
113 corresponds to a degree of saturation of 95% and a void ratio of 0.79). After the compaction  
114 of the first three layers, the pile was installed and the remaining soil was compacted around  
115 the pile by 100 mm thick layers. Attention was paid to ensure the homogeneity of soil next  
116 to the pile without touching the pile during soil compaction. Compaction layers are  
117 materialised using dashed lines in Figure 1. It should be noted that the average dry density of  
118 each compaction layer is controlled by the mass of soil used for compaction and the volume  
119 of the layer (thickness and diameter). Compacting the clay sample by several layers was  
120 chosen as an appropriate method to ensure its homogeneity prior to testing. Once  
121 compaction was finished, saturation was started by injecting water from the bottom of the  
122 container with a pressure of 20 kPa. To do so, the water tank was filled with water and its  
123 bottom was connected to the bottom of the soil container. At the end of the saturation, the  
124 level of water decrease and the final pressure was approximately 15 kPa. During this period,  
125 the water tank was blocked to avoid applying any force on the pile head. The soil surface  
126 was also covered with a thin layer of water and a plastic film to avoid water evaporation.  
127 This condition was maintained for 10 months until the estimated volume of water intake  
128 exceeded the initial air-filled pore volume. The soil was then assumed to be fully saturated.  
129 Measurement of the pile head displacement and visual inspection of the soil surface show  
130 that the soil surface did not move during saturation. Evaluation of the effects of saturation  
131 on the clay microstructure was not investigated. Note that Ng *et al.* (2014) consolidated  
132 kaolin clay slurry in order to obtain saturated clay sample for small-scale test but centrifuge  
133 was required to accelerate the consolidation process. In the present work, consolidation was  
134 not possible at 1-g condition. For this reason, compaction method was chosen to prepare  
135 the clay sample.

136 After saturation of the soil mass, the pile was first subjected to mechanical loading tests.  
137 Axial load was increased from 0 to 100 N, and then by increments of 50 N. Each increment  
138 was kept for 60 min. Loading was continued until failure, corresponding to a pile head  
139 settlement of 10% of the pile diameter (2 mm). Two mechanical tests, F1 and F2, were  
140 conducted using this loading procedure to check the repeatability of the experimental  
141 procedure. It should be noted that regarding the complexity of the compaction and  
142 saturation procedures, all the tests in this study were conducted on a single pile embedded  
143 at the centre of a single soil mass. This process was adopted following the work of Akrouch  
144 *et al.* (2014). An interval of two weeks between two subsequent mechanical tests was  
145 imposed to allow the equilibrium of stress state after each test. The initial states of the  
146 subsequent mechanical tests were then assumed to be similar.

147 After the mechanical tests, five thermo-mechanical tests were performed. Each test includes  
148 the following steps: (i) Increase of axial load to a given value which was maintained during  
149 the subsequent thermal cycle; (ii) Heating the pile from 22°C to 27°C; (iii) Cooling the pile to  
150 22°C; (iv) Cooling the pile to 17°C; (v) Heating the pile to its initial temperature (22°C); (vi)  
151 Remove the axial load at 22°C. The pile temperature was maintained at 22°C until the  
152 subsequent test started. Each step took 120 min, except the last one, which was longer (800  
153 min). Five thermo-mechanical tests, denoted by F3, F4, F5, F6 and F7, were performed at  
154 100 N, 150 N, 200 N, 250 N and 300 N, respectively. This procedure allowed starting all the  
155 thermo-mechanical tests at the same pile temperature (22°C) and the duration of the last  
156 step (800 min) was assumed to be long enough to ensure the recovery of the system. That  
157 allows also performing one test per 24h and the five tests (F3-F7) in a week.

### 158 **3. Experimental results**

159 As all the tests were performed using a single soil mass and a single model pile, the global  
1 response of the soil/pile system is first examined via load settlement curves of the entire  
2  
3 160 tests in Figure 3. The results show the permanent downward movement of the pile in the  
4  
5 161 soil, which is more explicit under purely mechanical loading (tests F1 and F2). From the  
6  
7 162 results of test F1 and considering 2 mm (10% of pile's outer diameter) as the pile settlement  
8  
9 163 at failure, the pile's resistance can be estimated at 500-550 N. Test F2 was stopped  
10  
11 164 intentionally before failure.  
12  
13  
14  
15  
16  
17

18  
19 166 In Figure 4, the load-settlement curves of the thermo-mechanical tests (F3 to F7), which  
20  
21 167 followed pile unloading in test F2, are shown at a larger scale. In each test, the pile response  
22  
23 168 exhibits approximately the same stiffness during mechanical loading. The pile continues to  
24  
25 169 settle during the applied thermal cycle under constant load. Unloading the pile leads to pile  
26  
27 170 heave. The slope of the unloading branch is the same in all thermo-mechanical tests, except  
28  
29 171 for test F4, which seems to be affected by a measurement problem. Also, the slope of the  
30  
31 172 unloading branch in test F2 is identical to the corresponding phase of other tests.  
32  
33  
34  
35  
36  
37

38 173 The pile behaviour in each individual test was then investigated. The pile settlement was  
39  
40 174 therefore zeroed (in the results analysis and not in the test) at the beginning of each test.  
41  
42 175 The pile head displacement curves of all the tests are plotted versus the pile head axial load  
43  
44 176 in Figure 5. The results relating to tests F3 to F7 are the pile response after the application of  
45  
46 177 the mechanical load and just before starting thermal cycling. A good repeatability of the  
47  
48 178 load-settlement curves can be observed, even when the figure is zoomed at a small range of  
49  
50 179 settlement (from 0 to 0.06 mm).  
51  
52  
53  
54  
55  
56

57 180 The results of mechanical test F1 are presented in Figure 6, where the pile head settlement  
58  
59 181 is plotted versus elapsed time for each loading step. That shows a quick settlement after the  
60  
61  
62  
63  
64  
65

182 load increase, followed by a stabilisation phase. As could be observed, for all the loading  
183 steps, the relationship between the settlement change and time (in a logarithmic scale) is  
184 linear under each loading step for  $t = 2$  to 60 min. The creep rate could then be determined  
185 from the slope of each curve in Figure 5, based on the French standard (Afnor, 1999).  
186 Following this standard, for each loading step, the creep rate is calculated as the change of  
187 pile head displacement between 2 and 60 min (of elapsed time) divided by  $\log(60/2)$ .

188 In Figure 7, the creep rate is plotted versus the axial load for all the tests. Note that in tests  
189 F1 and F2, the same procedure was followed (loading by steps), while in tests F3-F7, the  
190 target axial load was applied in one step. In spite of these different procedures, the  
191 relationships between the creep rate and the axial load are found to be similar in all tests;  
192 the creep rate increases quickly when the axial load exceeds 400 N. The fact that this rate  
193 depends only on the axial load and that it is independent of the loading path proves that it  
194 corresponds solely to creep and not to soil consolidation. After Edil & Mochtar (1988), the  
195 time-dependent displacement of a pile inserted in clay under a constant axial load is  
196 attributed primarily to creep of the pile-soil interface (slip) and shear creep of the soil  
197 surrounding the pile.

198 The load and the temperature of the pile measured in tests F3 to F7 are plotted in Figure 8.  
199 As explained above, from its initial temperature (around 22°C) after mechanical loading, the  
200 pile was heated to 27°C, cooled to 22°C, then cooled to 17°C, and finally heated to 22°C. The  
201 results show that the duration of each step (120 min) is long enough to bring the pile's  
202 temperature to the target value. During these heating/cooling steps, the pile head axial load  
203 was maintained constant (from  $t = 0$  to 600 min) by keeping the same water level in the  
204 water tank (see Figure 1). However the load measured by the force sensor appeared not to  
205 be perfectly constant. This blip in load reading can be explained by the small friction

206 between the rod, which transfers the water tank load to the pile head, and the frame that  
207 supports it. Heating the pile induces a pile head heave. In this case, the measured load  
208 corresponds to the water tank load plus the friction force. Inversely, cooling the pile induces  
209 a pile head settlement, and the load measured corresponds to the water tank load minus  
210 the friction force. These changes, in the order of a few Newtons, can be ignored in this  
211 study.

212 The results of tests F3-F7 are shown in Figure 9. Pile head settlement versus elapsed time is  
213 shown in Figure 9(a, c, e, g, i) for the whole test including mechanical loading, thermal cycle,  
214 and mechanical unloading. The pile settles under the mechanical load in the first 120 min of  
215 the test. It begins to heave while being heated from 22°C to 27°C. It settles during the  
216 subsequent cooling down to 17°C and heaves again during the last heating which increases  
217 the temperature back to 22°C. The final unloading (when the axial load is removed at t = 600  
218 min) induces a pile head heave. The time allocated to each thermal stage (120 min) may not  
219 be suitable for a relatively low-permeability material but the results show that the pile head  
220 displacement seems reached equilibrium at the end of each stage.

221 The change of pile head settlement versus change of temperature during the thermal cycle  
222 (between 120 min and 600 min in Figure 9a, c, e, g and i) is exhibited in Figure 9b, d, f, h, and  
223 j. The thermal expansion curve of an aluminium pile, having a fixed toe and being free to  
224 expand/contract in other directions, is also plotted. Its slope is equal to the linear thermal  
225 expansion coefficient of aluminium ( $23 \times 10^{-6}/^{\circ}\text{C}$ ). This representation is similar to that used  
226 by Kalantidou *et al.* (2012), Yavari *et al.* (2014), and Ng *et al.* (2014). The experimental  
227 results show that the pile reacts immediately to temperature change and heaves with the  
228 first heating; however its heave is smaller than that of the pile thermal expansion curve. It

229 settles when it is cooled. Under 100 N of axial load (Fig 8b), the slope of the cooling branch is  
230 close to that of the heating. This slope seems higher at higher pile head loads and looks  
231 similar to the pile thermal expansion curve under 300 N (Fig 8f). The pile heaves during the  
232 second heating phase; the slopes of the two heating branches are almost equal.

233 For further analysis of the pile displacement, the axial displacement distribution was plotted  
234 for each thermo-mechanical test (similar analysis have been done by Di Donna & Laloui,  
235 2015; Rotta Loria *et al.*, 2015). The end of the mechanical loading (start of 1<sup>st</sup> heating) was  
236 taken as the reference, with an axial displacement equal to zero along the pile. The first  
237 heating induced a pile head heave (in the figure, the axial displacement at 0 mm depth is  
238 taken equal to the measured pile head heave at the end of the first heating). The thermal  
239 expansion strain of the pile during this heating of 5°C is equal to  $5 \times 23 \times 10^{-6} = 115 \times 10^{-6}$ , where  
240  $23 \times 10^{-6}$  is the coefficient of thermal expansion of the pile. The stress change during heating  
241 along the pile was not measured in this study. However, as the pile head load was fixed  
242 during heating, the axial load along the pile can be reasonably assumed to be smaller than  
243 20% of the maximal load (300 N). This assumption can be justified from other tests under  
244 similar conditions, *i.e.* heating a floating pile under constant pile head load (Bourne-Webb *et*  
245 *al.*, 2009; Ng *et al.*, 2015). The maximal axial stress change (20% of the maximal load divided  
246 by the pile section) along the pile during heating can then be estimated as  
247  $20\% \times 300 / (0.01 \times 0.01 \times 3.14) = 19 \times 10^4$  Pa. That corresponds to an axial strain (axial stress  
248 divided by the pile equivalent Young modulus) of  $19 \times 10^4 / 13 \times 10^9 = 15 \times 10^{-6}$  (where  $13 \times 10^9$  Pa  
249 is the equivalent Young modulus of the pile following Yavari *et al.*, 2014a). This estimation  
250 shows that the axial displacement along the pile related to the stress change during heating  
251 can be ignored compared to the thermal expansion. The distribution of the axial  
252 displacement along the pile can then be estimated from the pile head displacement

253 (measured) and the pile thermal expansion calculated (see Figure 10). The results show that  
1  
2  
3 254 the pile toe settles during the first heating. The subsequent cooling induces heave at the pile  
4  
5 255 toe except the case of the highest pile head load (F7), where settlement of the pile toe was  
6  
7 256 observed. In addition, the higher the pile head load, the lower the pile toe's heave during  
8  
9  
10 257 cooling. The second heating induces a settlement at the pile toe for all the tests. These  
11  
12  
13 258 trends are similar to that observed by Pasten & Santamarina (2014), using numerical  
14  
15 259 modelling.

16  
17  
18  
19 260 In Figure 11, the pile head settlement induced by thermal cycling (between 120 min and 600  
20  
21 261 min) is plotted versus the applied pile head axial load for each test. From the creep rate,  
22  
23  
24 262 shown in Figure 6, the settlement related to the creep during this period can be estimated.  
25  
26 263 Note that Cui *et al.* (2009) showed that the temperature can significantly influence the time  
27  
28  
29 264 dependent behaviour of clay but their tests were performed in a large range of temperature  
30  
31  
32 265 (from 25°C to 80°C). In the present work, the temperature change is much smaller (from  
33  
34 266 17°C to 27°C) and the pile head settlement related to creep (smaller than 0.005 mm for each  
35  
36  
37 267 period) is small compared to that related to the mechanical loading (see Figure 11). As a  
38  
39  
40 268 consequence, effects of temperature on creep settlement can be ignored. The settlement  
41  
42 269 directly related to the thermal cycle can then be estimated: corrected value is the measured  
43  
44  
45 270 value minus the creep value (calculated from isothermal mechanical tests, see Figure 7). The  
46  
47 271 results show that the settlement related to the thermal cycle is higher when the pile is  
48  
49  
50 272 subjected to a higher axial load.

#### 53 273 **4. Discussion**

54  
55  
56 274 The results obtained on the mechanical loading part (Figures 5 and 7) show a good  
57  
58 275 repeatability between the tests. The same settlement curve of the pile in all tests indicates  
59  
60  
61  
62  
63  
64  
65

276 that the behaviour of the pile in one test is independent of the previous one. That suggests  
277 that the soil/pile system could have retrieved its initial equilibrium condition prior to the  
278 subsequent test. Actually, the pile has been loaded to failure during test F1 (Figure 3). For  
279 the subsequent test (F2), the pile shaft resistance would decrease due to the possible  
280 softening of the shear behaviour at the clay/pile interface (see Di Donna *et al.* 2016; Yavari  
281 *et al.* 2016). On the contrary, the pile toe resistance would increase if the clay consolidates  
282 after test F1. On one hand, the two mechanisms have opposite effects on the pile response;  
283 on the other hand, they could be negligible (because the clay has been already well  
284 compacted and the softening observed on a similar material by Yavari *et al.* 2016 is quite  
285 small under low stresses). That would explain why the mechanical response of the pile  
286 during test F2 is quite similar to that during test F1 (see Figure 5), suggesting that the waiting  
287 stage after failure test is sufficient for the clay to recover its initial mechanical properties.  
288 The choice of performing various tests in a unique mass of saturated clay can thus be  
289 considered as an appropriate one.

290 It should be noted that the irreversible settlement observed during the thermal cycle is  
291 larger at a higher axial load. While testing dry sand, Kalantidou *et al.* (2012) and Yavari *et al.*  
292 (2014b) found that the effect of thermal cycle under constant axial load was reversible under  
293 low loads (smaller than 30% of the pile resistance) and irreversible under high loads. In the  
294 present work, where tests were performed within a wide range of axial load (from 20% to  
295 60% of the pile's resistance), irreversible settlement is observed even at low loads (100 N  
296 corresponds to less than 20% of the pile resistance, which is between 500 and 550 N). Ng *et*  
297 *al.* (2014) have also observed irreversible settlement after thermal cycles under constant  
298 load at 40% of the pile's resistance. However, in the work of Ng *et al.* (2014), thermo-  
299 mechanical ratcheting was observed to level off after few thermal cycles. In the present

300 work, only one thermal cycle was applied and such phenomenon could not be observed.

301 Concerning accumulated thermal displacement, Ng *et al.* (2014) obtained 2.1% and 3.8% of  
302 pile diameter after five cycles. In the present work, the irreversible thermal settlement  
303 obtained after one cycle was smaller than 0.5% of the pile diameter, which is in agreement  
304 with the work of Ng *et al.* (2014).

305 Beside experimental works, irreversible settlement of energy piles subjected to thermal  
306 cycles has also been investigated through numerical modelling. Suryatriyastuti *et al.* (2014)  
307 used a load transfer approach to study the cyclic behaviour of energy pile and found that  
308 thermo-mechanical ratcheting observed under thermal cycle could be predicted by  
309 considering a cyclic strain hardening/softening mechanism at the soil/pile interface.  
310 However, in the work of Pasten & Santamarina (2014), the main features of energy piles  
311 subjected to static load and thermal cycles (i.e. irreversible settlement after thermal cycles  
312 and displacement accumulation depending on the static factor of safety) were reproduced  
313 by numerical simulations without considering the cyclic strain hardening/softening  
314 mechanism. Actually, the authors explained the irreversible settlement by the decrease of  
315 mobilised shaft shear stress with thermal cycles. Saggi & Chakraborty (2015) simulated the  
316 cyclic thermo-mechanical behaviour of a floating energy pile in sand, and found an  
317 irreversible settlement only for the first heating/cooling cycle. The subsequent cycles induce  
318 an irreversible uplift of the pile.

319 In the present work, only one heating/cooling cycle was applied for each loading step.  
320 Thermo-mechanical ratcheting was observed for all the tests. In addition, this settlement is  
321 higher at a higher mechanical load. The mechanisms by which thermal cycles affect the pile  
322 behaviour can be explained from the profile of axial displacement shown in Figure 10.

1  
2  
3  
4  
5  
6  
7  
8  
9  
10  
11  
12  
13  
14  
15  
16  
17  
18  
19  
20  
21  
22  
23  
24  
25  
26  
27  
28  
29  
30  
31  
32  
33  
34  
35  
36  
37  
38  
39  
40  
41  
323 Actually, after the mechanical loading, the first heating induces a pile expansion. This latter  
324 corresponds to a pile head heave (that was measured from the experiments) and a pile toe  
325 settlement. The pile toe settlement is induced by the reduction of the pile shaft resistance,  
326 which increases the load transfer to the pile toe (see Pasten & Santamarina, 2014). The  
327 subsequent cooling induces a pile contraction, which induces a pile head settlement  
328 (measured experimentally) and a pile toe heave (except for the case at high load, F7, where  
329 a pile toe settlement was expected). It should be also noted that the pile toe heave during  
330 cooling is lower at a higher mechanical load. Finally, the second heating, which brings the  
331 pile back to its initial temperature, induces again a pile toe settlement. The total pile toe  
332 settlement after the thermal cycle is positive and higher at a higher mechanical load. To  
333 explain these results, the pile toe settlement can be attributed to two mechanisms: (i) the  
334 compression of the clay below the pile toe; (ii) the displacement of the pile related to  
335 shearing of the clay surrounding the pile toe. If the first mechanism can be expected to be  
336 almost reversible, the second one is most likely irreversible. The observed thermo-  
337 mechanical ratcheting can then be attributed to the second mechanism (shearing of the clay  
338 surrounding the pile toe).

42  
43  
44  
45  
46  
47  
48  
49  
50  
51  
52  
53  
54  
55  
56  
57  
58  
59  
60  
61  
62  
63  
64  
65  
339 The thermally induced irreversible settlement could become significant in the design of  
340 energy piles in saturated clay. When all the piles of the foundation are equipped with the  
341 heat exchanger system, additional settlement of the foundation can be expected with  
342 seasonal temperature change of piles. When only a part of foundation piles is equipped with  
343 the heat exchanger system, cycles of temperature applied to these piles would reduce  
344 progressively their axial load while the axial load in the non-equipped piles increases, thus  
345 leading to redistributions of loads among the different piles.

## 346 **5. Conclusion**

1  
2 347 Thermo-mechanical loading was applied to a model pile in saturated clay. The pile head axial  
3  
4  
5 348 load, displacement and temperature were monitored. Analysis of the experimental results  
6  
7 349 shows that:

10  
11 350 - Under mechanical loading, the creep rate (of the pile head displacement) increases as  
12  
13 351 the pile head load approaches to pile ultimate resistance but remains negligible at  
14  
15  
16 352 low pile head load.

18  
19 353 - Under a constant pile head axial load, heating the pile induces pile head heave while  
20  
21  
22 354 cooling induces settlement. This behaviour is mainly related to the thermal  
23  
24  
25 355 expansion/contraction of the pile.

26  
27  
28 356 - Irreversible settlement of the pile head is observed after the heating/cooling cycle  
29  
30  
31 357 under constant pile head axial load. This settlement is larger under higher axial loads,  
32  
33 358 and is much more significant than that due to creep under isothermal conditions.

34  
35  
36  
37 359 The findings of this study, observed on a model pile, would be helpful when considering the  
38  
39  
40 360 long-term mechanical behaviour in the design of energy piles in saturated clay. Actually,  
41  
42 361 seasonal piles temperature change could induce additional settlement of the foundation or  
43  
44  
45 362 redistribution of foundation load on the piles.

## 47 363 **6. Acknowledgement**

48  
49  
50 364 The authors would like to express their great appreciation to the French National Research  
51  
52  
53 365 Agency for funding the present study, which is part of the project PiNRJ “Geotechnical  
54  
55  
56 366 aspects of foundation energy piles” – ANR 2010 JCJC 0908 01.

## 59 367 **7. References**

- 368 Abuel-Naga, H.M., Bergado, D.T., Bouazza, A. & Ramana, G.V. (2007). Volume change  
behaviour of saturated clays under drained heating conditions : experimental results  
and constitutive modeling. *Canadian Geotechnical Journal* **44**, 942 – 956.
- 371 AFNOR (1999). Essai statique de pieu sous effort axial. NF P 94-150.
- 372 Akrouch, G., Sánchez, M. & Briaud, J. (2014). Thermo-mechanical behavior of energy piles in  
high plasticity clays. *Acta Geotechnica* **6**, 503–519.
- 374 Amatya, B. L., Soga, K., Bourne-Webb, P. J., Amis, T. & Laloui, L. (2012). Thermo-mechanical  
behaviour of energy piles. *Géotechnique* **62**, No. 6, 503–519.
- 376 Bourne-Webb, P. J., Amatya, B., Soga, K., Amis, T., Davidson, C. & Payne, P. (2009). Energy  
pile test at Lambeth College, London: geotechnical and thermodynamic aspects of pile  
response to heat cycles. *Géotechnique* **59** No. 3, 237–248.
- 379 Brandl, H. (2006). Energy foundations and other thermo-active ground structures.  
*Géotechnique* **56**, No. 2, 81–122.
- 381 Brandl, H. (2013). Thermo-active ground-source structures for heating and cooling. *Procedia  
Engineering* **57**, 9–18.
- 383 Cekerevac, C. & Laloui, L. (2004). Experimental study of thermal effects on the mechanical  
behaviour of a clay. *International Journal for Numerical and Analytical Methods in  
Geomechanics* **28**, 209–228.
- 386 Cui, Y.J., Le, T.T., Tang, A.M., Delage, P. & Li, X.L. (2009). Investigating the time-dependent  
behaviour of Boom clay under thermomechanical loading. *Géotechnique* **59**, No. 4, 319  
– 329.

- 389 De Moel, M., Bach, P. M., Bouazza, A., Singh, R. M. & Sun, J. O. (2010). Technological  
1  
2  
3 390 advances and applications of geothermal energy pile foundations and their feasibility  
4  
5 391 in Australia. *Renewable and Sustainable Energy Reviews* **14**, No. 9, 2683–2696.  
6  
7  
8  
9 392 Di Donna, A & Laloui, L. (2013). Advancements in the Geotechnical Design of Energy Piles.  
10  
11 393 *International Workshop on Geomechanics and Energy*, (November 2013), 26–28.  
12  
13  
14  
15 394 Di Donna, A. & Laloui, L. (2015). Numerical analysis of the geotechnical behaviour of energy  
16  
17 395 piles. *Int. J. Numer. Anal. Meth. Geomech.* **39**, 861 – 888.  
18  
19  
20  
21 396 Di Donna, A., Ferrari, A. & Laloui, L. (2016). Experimental investigation of the soil-concrete  
22  
23 397 interface: physical mechanisms, cyclic mobilisation and behaviour at different  
24  
25  
26 398 temperatures. *Canadian Geotechnical Journal* (doi: 10.1139/cgj-2015-0294).  
27  
28  
29 399 Edil, T.B. & Mochtar, I.B. (1988). Creep response of model pile in clay. *Journal of*  
30  
31  
32 400 *Geotechnical Engineering* **114**, No. 11, 1245 – 1260.  
33  
34  
35 401 Hong, P. Y., Pereira, J. M., Tang, A. M. & Cui, Y. J. (2013). On some advanced thermo-  
36  
37  
38 402 mechanical models for saturated clays. *International Journal for Numerical and*  
39  
40  
41 403 *Analytical Methods in Geomechanics* **37**, No. 17, 2952–2971.  
42  
43  
44 404 Hueckel, T., Francois, B. & Laloui, L. (2011). Temperature-dependent internal friction of clay  
45  
46  
47 405 in a cylindrical heat source problem. *Géotechnique*, **61**, No. 10, 831–844.  
48  
49  
50 406 Kalantidou, A., Tang, A. M., Pereira, J.-M. & Hassen, G. (2012). Preliminary study on the  
51  
52  
53 407 mechanical behaviour of heat exchanger pile in physical model. *Géotechnique* **62**, No.  
54  
55 408 11, 1047–1051.  
56  
57  
58  
59  
60  
61  
62  
63  
64  
65

- 409 Laloui, L., Moreni, M. & Vulliet, L. (2003). Comportement d'un pieu bi-fonction, fondation et  
1 échangeur de chaleur. *Canadian Geotechnical Journal* **40**, No. 2, 388–402.  
2  
3  
4  
5  
6 411 Laloui, L., Nuth, M. & Vulliet, L. (2006). Experimental and numerical investigations of the  
7  
8 412 behaviour of a heat exchanger pile. *International Journal for Numerical and Analytical*  
9  
10  
11 413 *Methods in Geomechanics* **30**, No. 8, 763–781.  
12  
13  
14 414 Laloui, L., Olgun, C. G., Sutman, M., McCartney, J. S., Coccia, C. J., Abuel-Naga, H. M. &  
15  
16  
17 415 Bowers, G. A. (2014). Issues involved with thermoactive geotechnical systems:  
18  
19 416 characterization of thermomechanical soil behavior and soil-structure interface  
20  
21  
22 417 behavior. *DFI Journal: The Journal of the Deep Foundations Institute* **8**, No. 2, 108–120.  
23  
24  
25  
26 418 McCartney, J. S. & Murphy, K. D. (2012). Strain Distributions in Full-Scale Energy Foundations  
27  
28 419 ( DFI Young Professor Paper Competition 2012 ). *DFI Journal: The Journal of the Deep*  
29  
30  
31 420 *Foundations Institute* **6**, No. 2, 26–38.  
32  
33  
34 421 Mimouni, T. & Laloui, L. (2014). Towards a secure basis for the design of geothermal piles.  
35  
36  
37 422 *Acta Geotechnica* **9**, 355 – 366.  
38  
39  
40 423 Muhammed, R.D. (2015). *Etude en chambre d'étalonnage du frottement sol-pieu sous grands*  
41  
42  
43 424 *nombres de cycles. Applications au calcul des fondations profondes dans les sols fins*  
44  
45  
46 425 *saturés*. PhD thesis of Université Pierre Marie Curie, 204 pages.  
47  
48  
49 426 Murphy, K. D. & McCartney, J. S. (2014). Thermal Borehole Shear Device. *Geotechnical*  
50  
51  
52 427 *Testing Journal* **37**, No. 6, 20140009.  
53  
54  
55 428 Murphy, K. D., McCartney, J. S. & Henry, K. S. (2014). Evaluation of thermo-mechanical and  
56  
57  
58 429 thermal behavior of full-scale energy foundations. *Acta Geotechnica* **10**, 179-195.  
59  
60  
61  
62  
63  
64  
65

- 1  
2  
3 430 Ng, C. W. W., Shi, C., Gunawan, A. & Laloui, L. (2014). Centrifuge modelling of energy piles  
4  
5  
6 431 subjected to heating and cooling cycles in clay. *Géotechnique Letters* **4**, 310 –316.  
7  
8  
9 432 Ng, C. W. W., Shi, C., Gunawan, A., Laloui, L. & Liu, H.L. (2015). Centrifuge modelling of  
10  
11 433 heating effects on energy pile performance in saturated sand. *Can. Geotech. J.* **52**,  
12  
13 434 1045 – 1057.  
14  
15 435 Olgun, C.G., Ozudogru, T.Y., Abdelaziz, S.L. & Senol, A. (2014). Long-term performance of  
16  
17 436 heat exchanger piles. *Acta Geotechnica* **10**, No. 5, 553 – 569.  
18  
19  
20 437 Pasten, C. & Santamarina, C. (2014). Thermally Induced Long-Term Displacement of  
21  
22 438 Thermoactive Piles. *J. Geotech. Geoenviron. Eng.*, **140**(5): 06014003  
23  
24  
25  
26 439 Péron, H., Knellwolf, C. & Laloui, L. (2011). A method for the geotechnical design of heat  
27  
28 440 exchanger piles. *Geo-Frontiers 2011*, 470–479.  
29  
30  
31  
32 441 Rotta Loria, A.F., Gunawan, A., Shi, C., Laloui, L. & Ng, W.W.C. (2015). Numerical modelling of  
33  
34 442 energy piles in saturated sand subjected to thermo-mechanical loads. *Geomechanics*  
35  
36 443 *for Energy and the Environment* **1**, 1 – 15.  
37  
38  
39  
40  
41 444 Saggiu, R. & Chakraborty, T. (2015). Cyclic Thermo-Mechanical Analysis of Energy Piles in  
42  
43 445 Sand. *Geotech Geol Eng* **33**, 321–342  
44  
45  
46  
47 446 Stewart, M.A. & McCartney, J.S. (2013). Centrifuge modelling of soil-structure interaction in  
48  
49 447 energy foundations. *Journal of Geotechnical and Geoenvironmental Engineering* **140**,  
50  
51 448 No. 4, 04013044.  
52  
53  
54  
55  
56 449 Suryatriyastuti, M.E., Mroueh, H. & Burlon, B., 2014. A load transfer approach for studying  
57  
58 450 the cyclic behavior of thermo-active piles. *Computers & Geotechnics* **55**, 378 – 391.  
59  
60  
61  
62  
63  
64  
65

1  
2  
3  
4  
5  
6  
7  
8  
9  
10  
11  
12  
13  
14  
15  
16  
17  
18  
19  
20  
21  
22  
23  
24  
25  
26  
27  
28  
29  
30  
31  
32  
33  
34  
35  
36  
37  
38  
39  
40  
41  
42  
43  
44  
45  
46  
47  
48  
49  
50  
51  
52  
53  
54  
55  
56  
57  
58  
59  
60  
61  
62  
63  
64  
65

451 Wang, B., Bouazza, A. & Haberfield, C. (2011). Preliminary observation from laboratory scale  
452 model geothermal pile subjected to thermo-mechanical loading. *Geo-Frontiers 2011*,  
453 430 – 439.

454 Wang, B., Bouazza, A., Singh, R. M., Haberfield, C., Barry-macaulay, D. & Baycan, S. (2014).  
455 Posttemperature Effects on Shaft Capacity of a Full-Scale Geothermal Energy Pile.  
456 *Journal of Geotechnical and Geoenvironmental Engineering* **141**, No. 4, 04014125.

457 Yavari, N., Tang, A. M., Pereira, J.-M. & Hassen, G. (2014a). A simple method for numerical  
458 modelling of energy pile’s mechanical behaviour. *Géotechnique Letters* **4**, 119–124.

459 Yavari, N., Tang, A. M., Pereira, J.-M. & Hassen, G. (2014b). Experimental study on the  
460 mechanical behaviour of a heat exchanger pile using physical modelling. *Acta*  
461 *Geotechnica* **9**, No. 3, 385 – 398.

462 Yavari, N., Tang, A. M., Pereira, J.-M. & Hassen, G. (2016). Effect of temperature on the shear  
463 shear strength of soils and soil/structure interface. *Canadian Geotechnical Journal* (doi:  
464 10.1139/cgj-2015-0355)

465

466

467 **List of captions**

1  
2  
3  
4  
5  
6  
7  
8  
9  
10  
11  
12  
13  
14  
15  
16  
17  
18  
19  
20  
21  
22  
23  
24  
25  
26  
27  
28  
29  
30  
31  
32  
33  
34  
35  
36  
37  
38  
39  
40  
41  
42  
43  
44  
45  
46  
47  
48  
49  
50  
51  
52  
53  
54  
55  
56  
57  
58  
59  
60  
61  
62  
63  
64  
65

468 Figure 1. Experimental set-up

469 Figure 2. Grain size distribution curve of kaolin clay

470 Figure 3. Pile load-settlement curve obtained through 7 successive tests F1 to F7

471 Figure 4. Pile load-settlement curve obtained through tests F3 to F7

472 Figure 5. Load-settlement curves for the mechanical phase

473 Figure 6. Results of test F1 – Pile head settlement versus elapsed time for each loading step

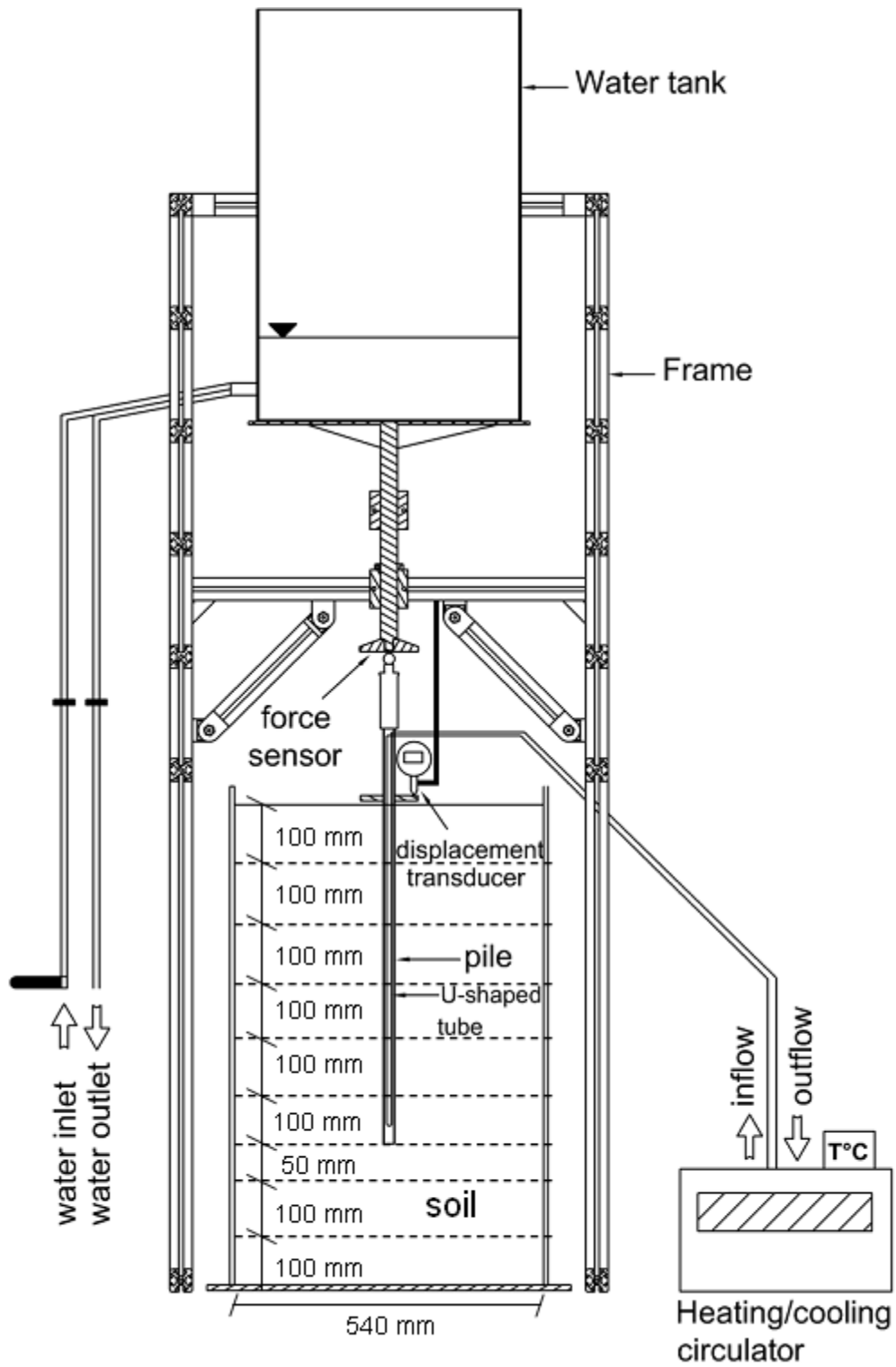
474 Figure 7. Creep rate versus axial load for the mechanical phase

475 Figure 8. Axial load and temperature of the pile in tests: (a) F3; (b) F4; (c) F5; (d) F6; (e) F7.

476 Figure 9. Results of tests F3-F7 for the thermal phase – Pile head settlement and pile temperature  
477 change: (a, b) F3; (c, d) F4; (e, f) F5; (g, h) F6; (i, J) F7.

478 Figure 10. Results of tests F3-F7 for the thermal phase - Axial displacement along the pile: (a) F3; (b)  
479 F4; (c) F5; (d) F6; (e) F7.

480 Figure 11. Results of tests F3-F7 for the thermal phase - Pile head settlement versus pile head axial  
481 load



482

483 **Figure 1. Experimental set-up**

484  
485  
486  
487  
488  
489  
490  
491  
492  
493  
494  
495  
496  
497  
498  
499  
500  
501  
502  
503  
504  
505  
506  
507  
508  
509  
510  
511  
512  
513  
514  
515  
516  
517  
518  
519  
520  
521  
522  
523  
524  
525  
526  
527  
528  
529  
530  
531  
532  
533  
534  
535  
536  
537  
538  
539  
540  
541  
542  
543  
544  
545  
546  
547  
548  
549  
550  
551  
552  
553  
554  
555  
556  
557  
558  
559  
560  
561  
562  
563  
564  
565

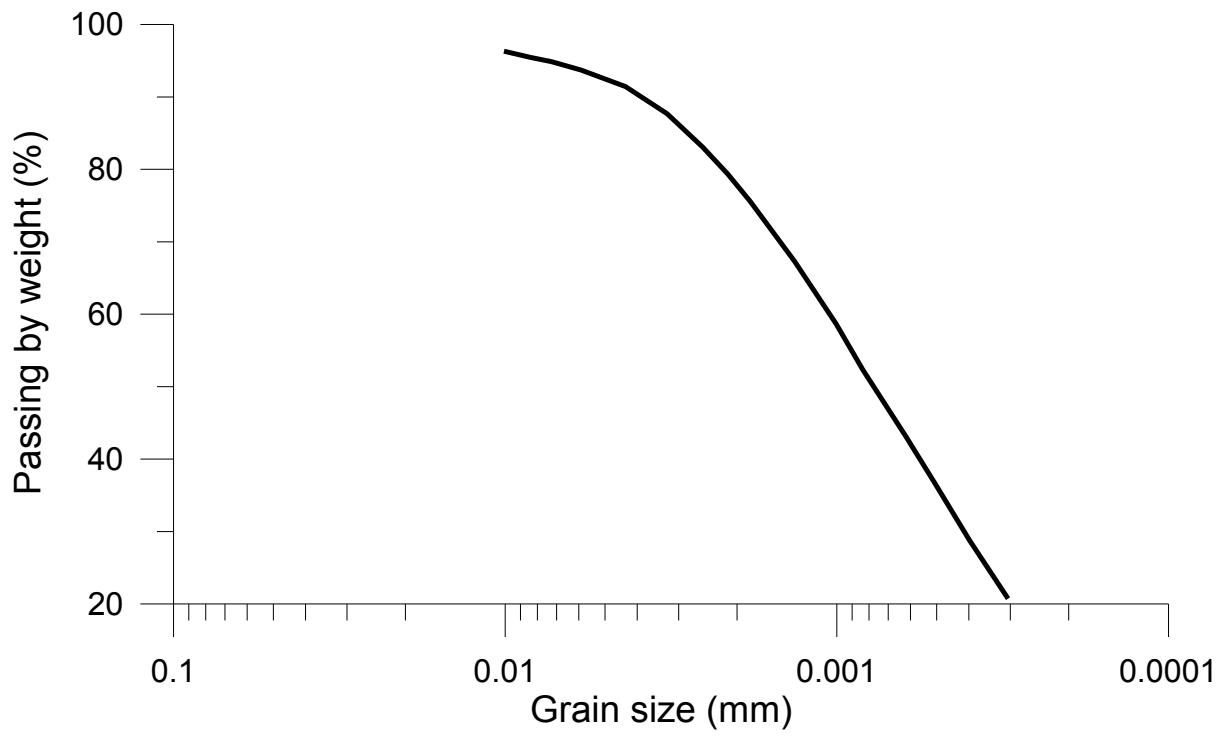


Figure 2. Grain size distribution curve of kaolin clay

1  
2  
3  
4  
5  
6  
7  
8  
9  
10  
11  
12  
13  
14  
15  
16  
17  
18  
19  
20  
21  
22  
23 484  
24  
25 485  
26  
27 486  
28  
29 487  
30  
31 488  
32  
33 489  
34  
35  
36 490  
37  
38  
39  
40  
41  
42  
43  
44  
45  
46  
47  
48  
49  
50  
51  
52  
53  
54  
55  
56  
57  
58  
59  
60  
61  
62  
63  
64  
65

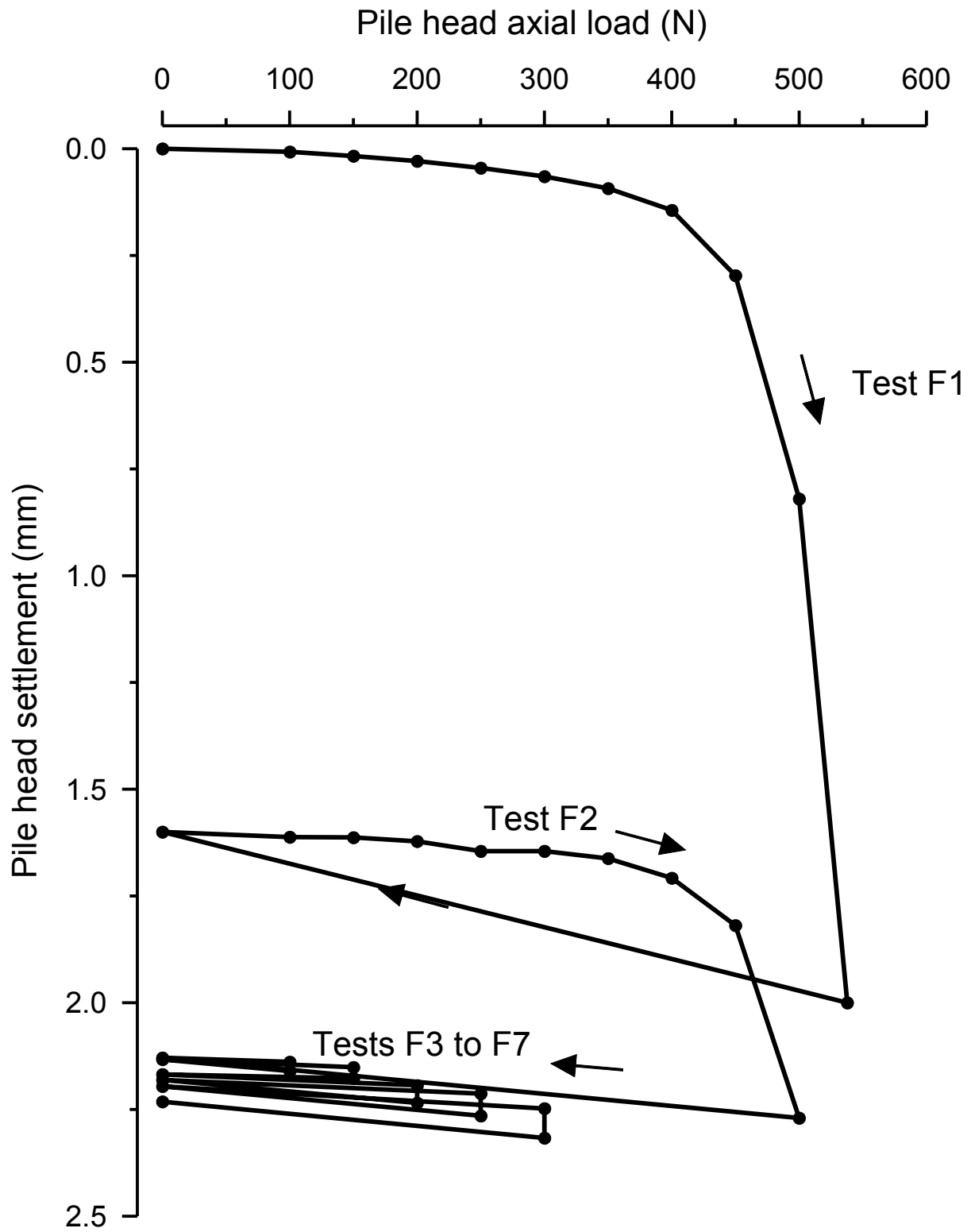


Figure 3. Pile load-settlement curve obtained through 7 successive tests F1 to F7

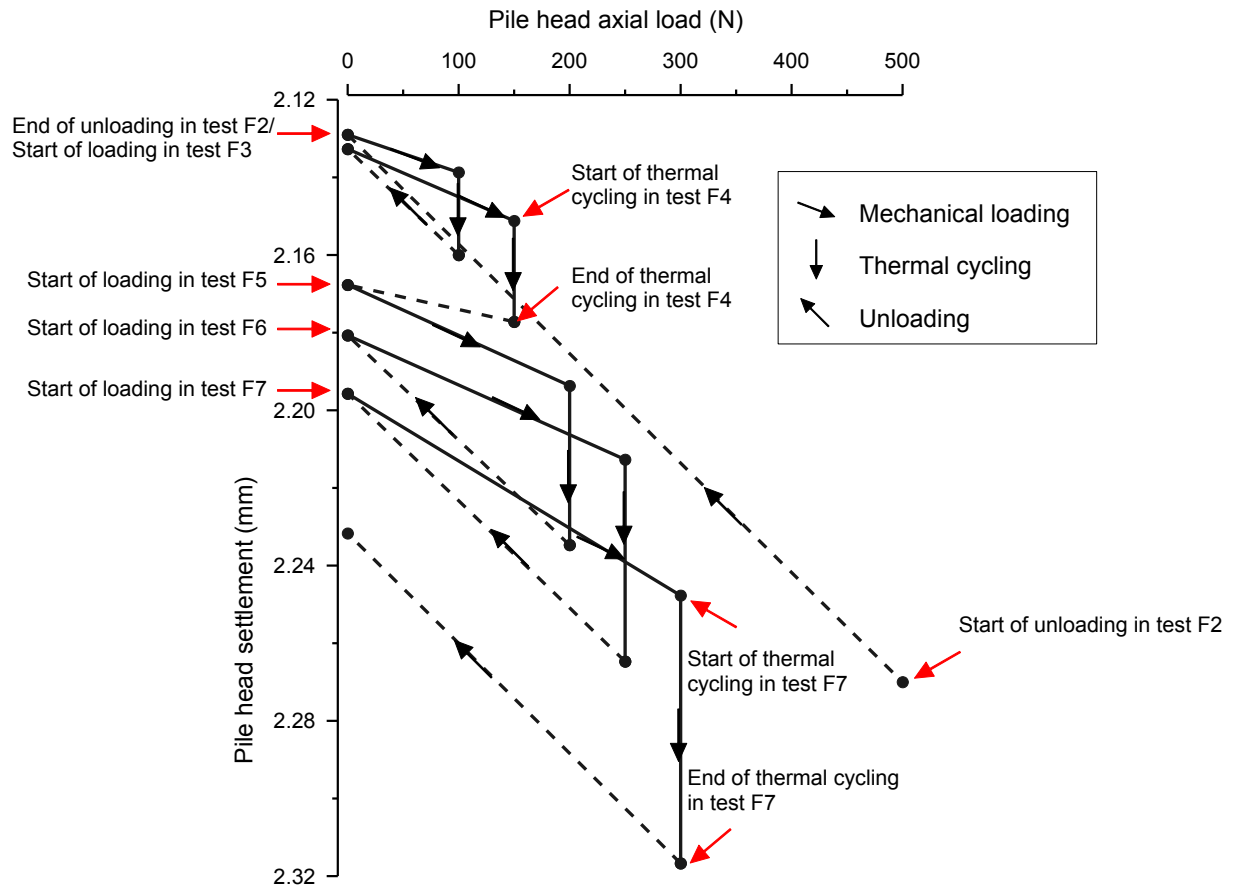


Figure 4. Pile load-settlement curve obtained through tests F3 to F7

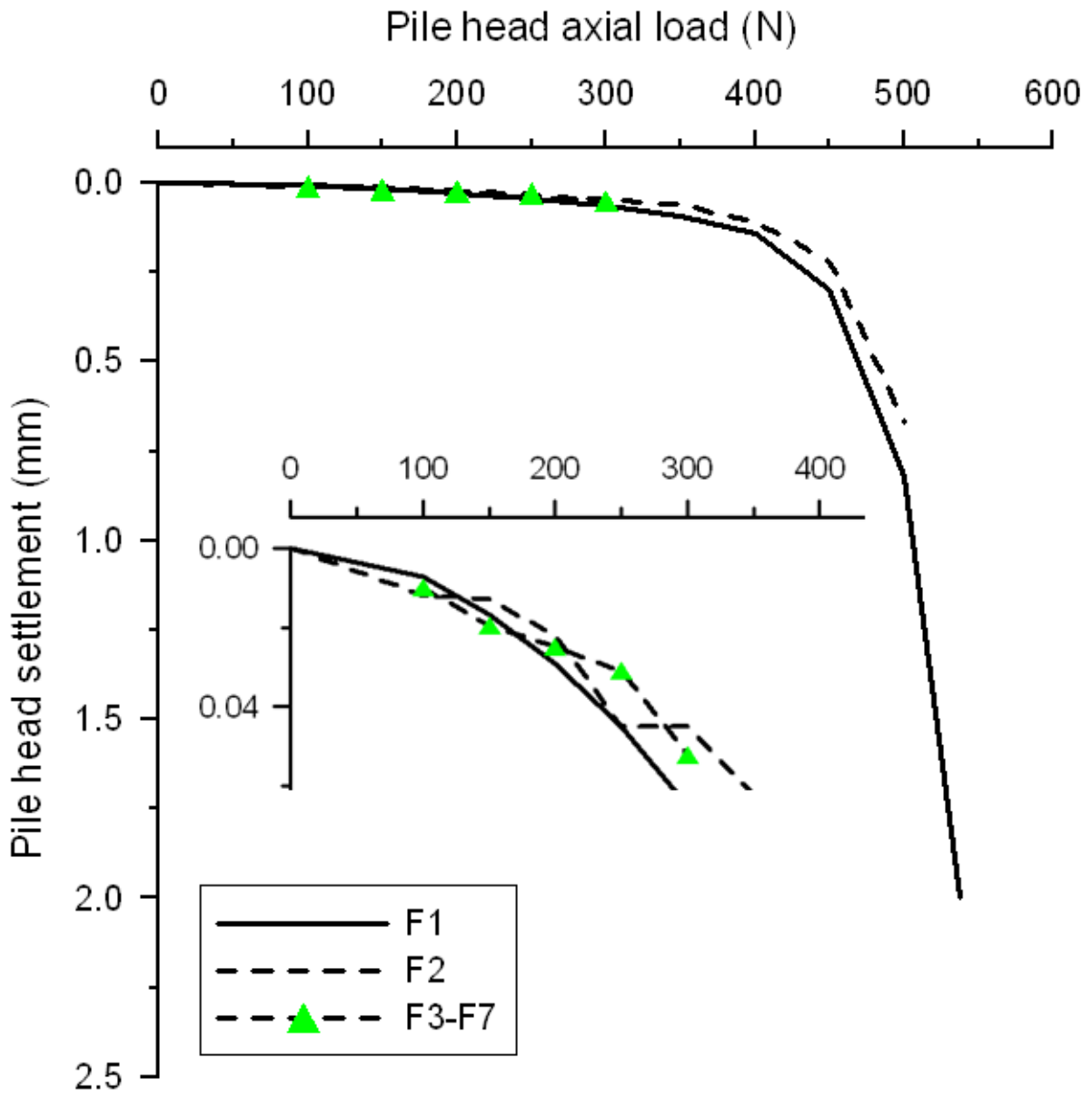


Figure 5. Load-settlement curves for the mechanical phase

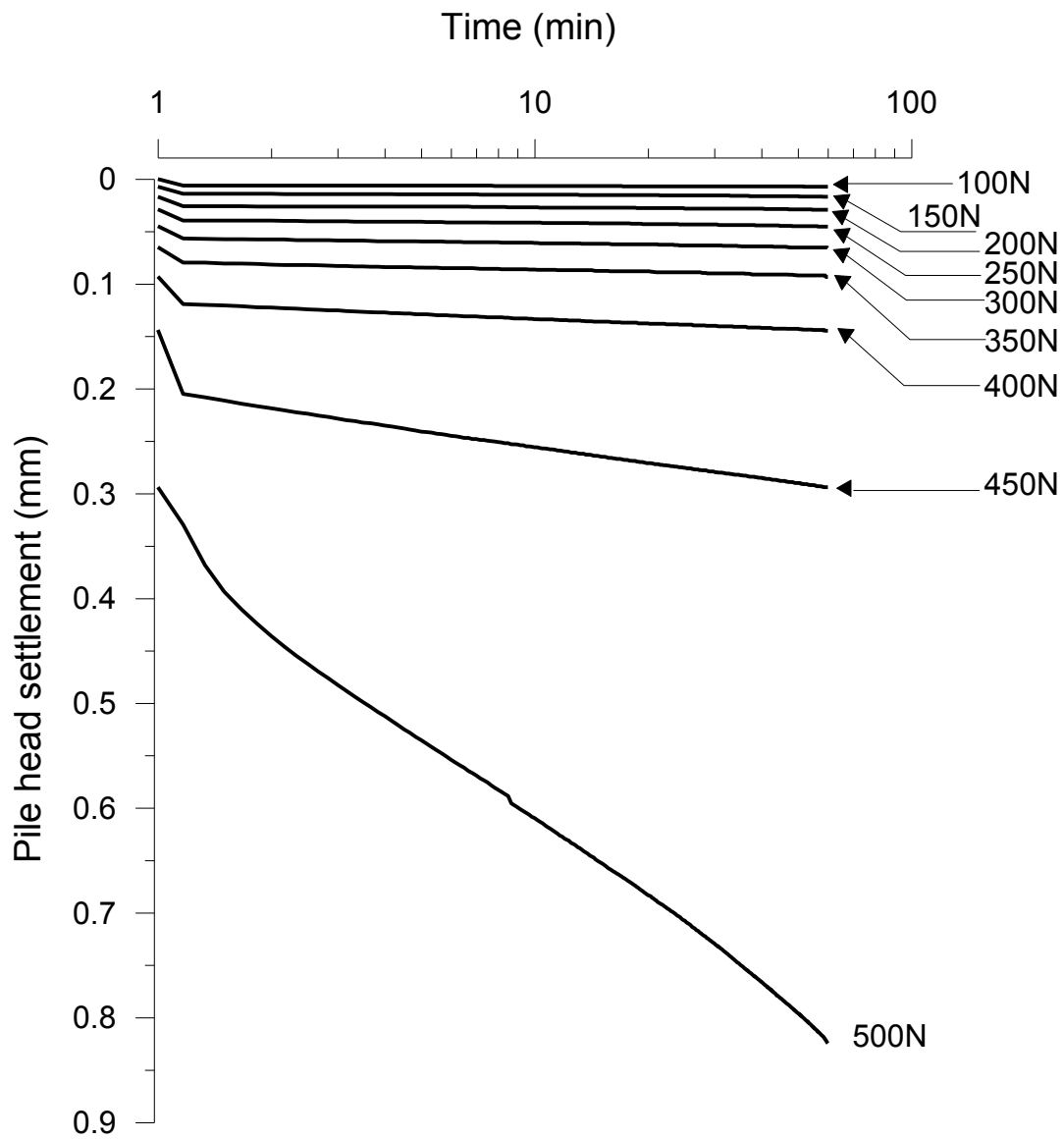


Figure 6. Results of test F1 – Pile head settlement versus elapsed time for each loading step

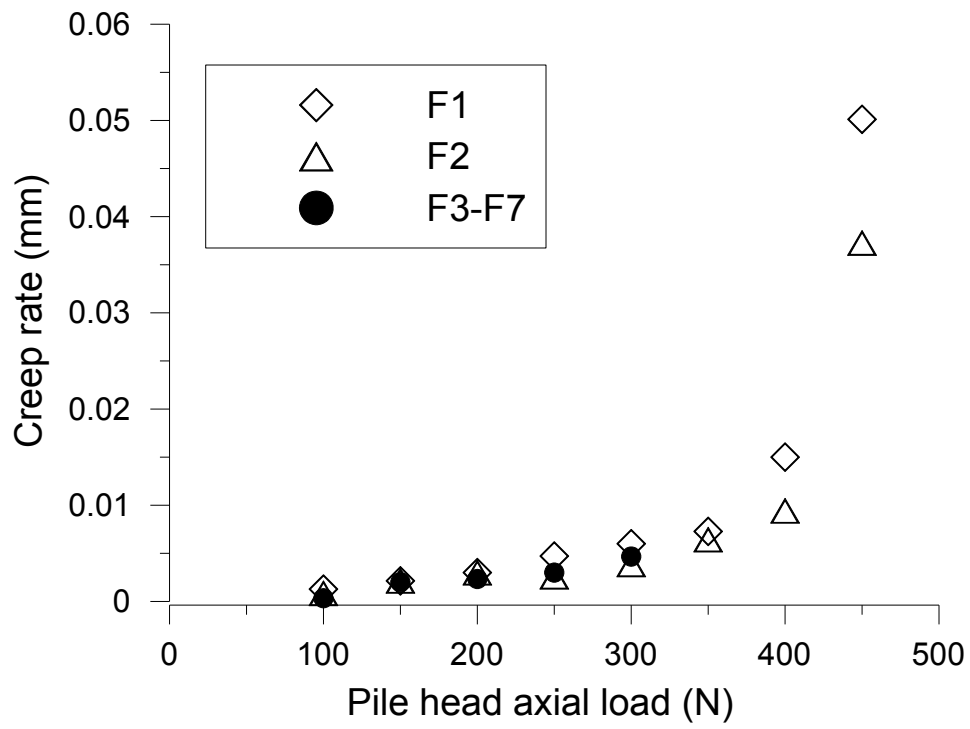


Figure 7. Creep rate versus axial load for the mechanical phase

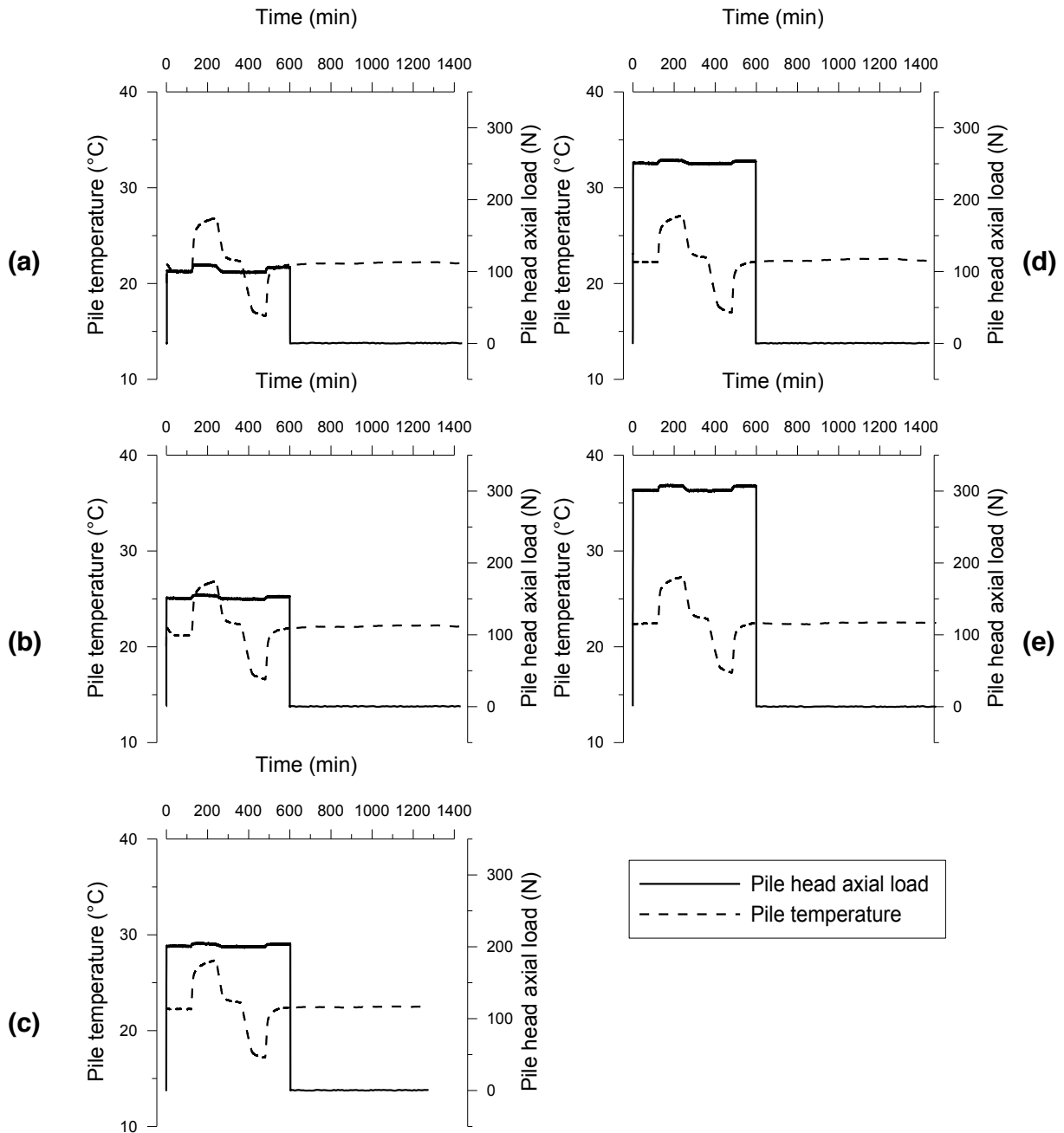
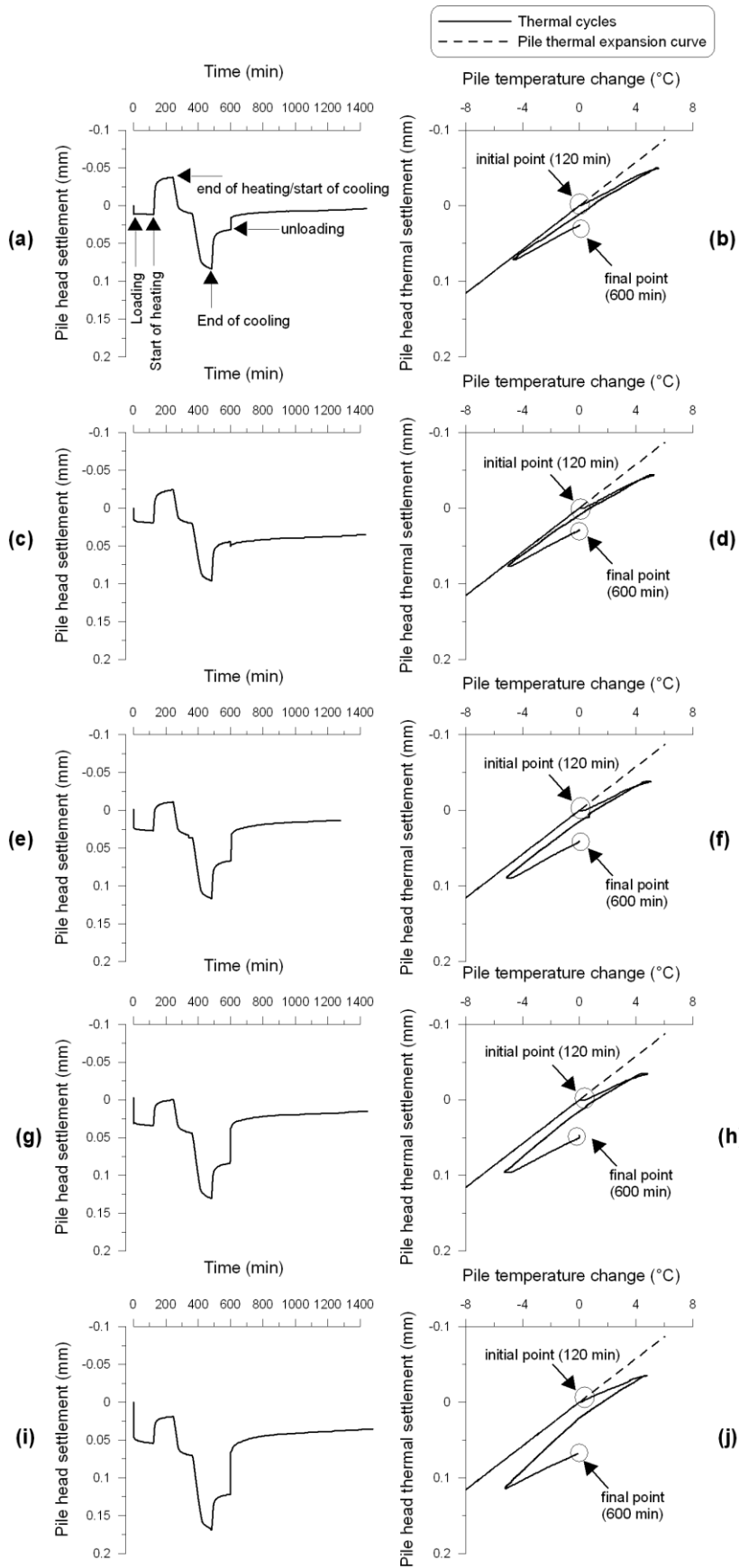
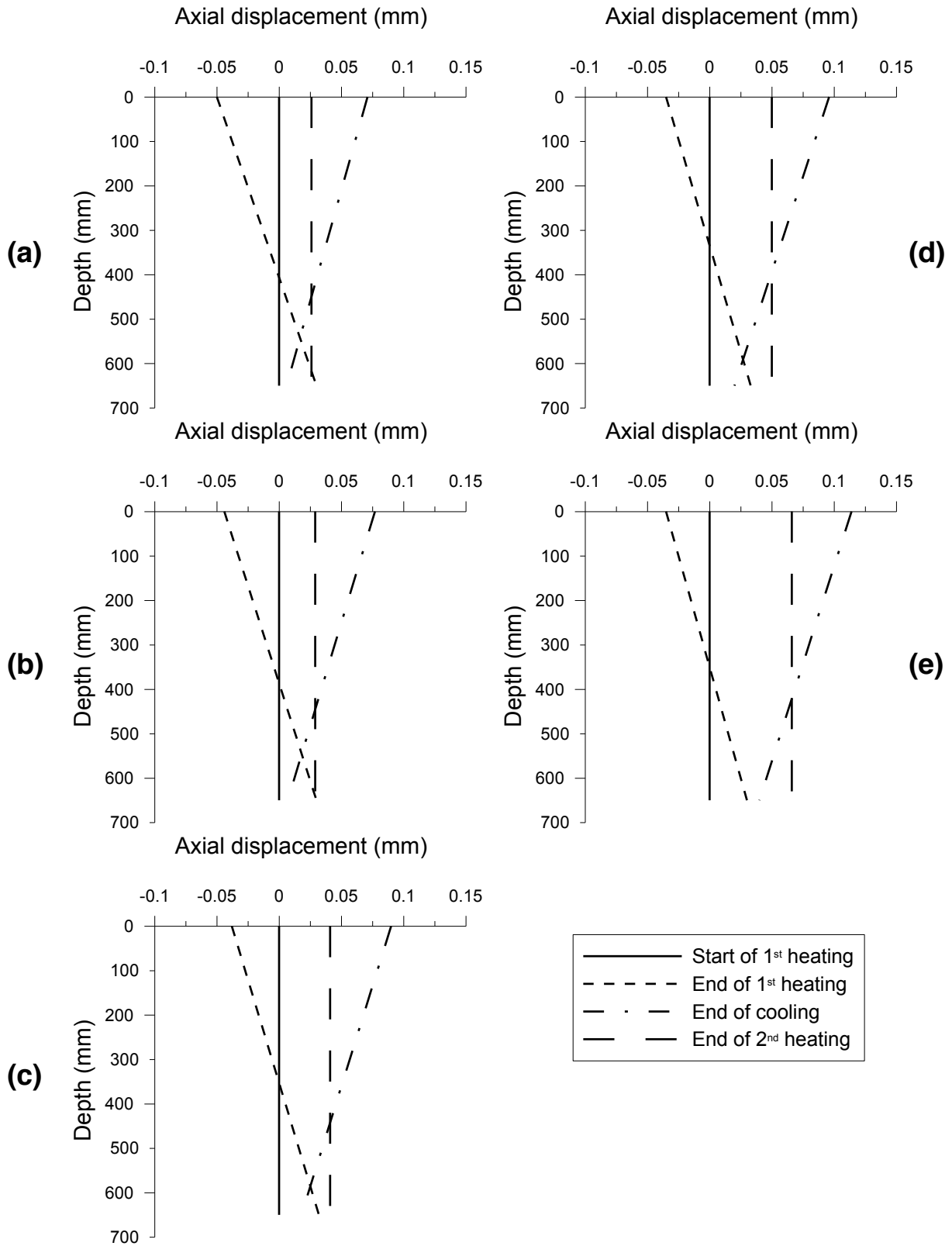


Figure 8. Axial load and temperature of the pile in tests: (a) F3; (b) F4; (c) F5; (d) F6; (e) F7.



512

513 **Figure 9. Results of tests F3-F7 for the thermal phase – Pile head settlement and pile temperature change: (a,**  
 514 **b) F3; (c, d) F4; (e, f) F5; (g, h) F6; (i, J) F7.**



516 **Figure 10. Results of tests F3-F7 for the thermal phase - Estimated axial displacement along the pile: (a) F3;**  
 517 **(b) F4; (c) F5; (d) F6; (e) F7.**

518

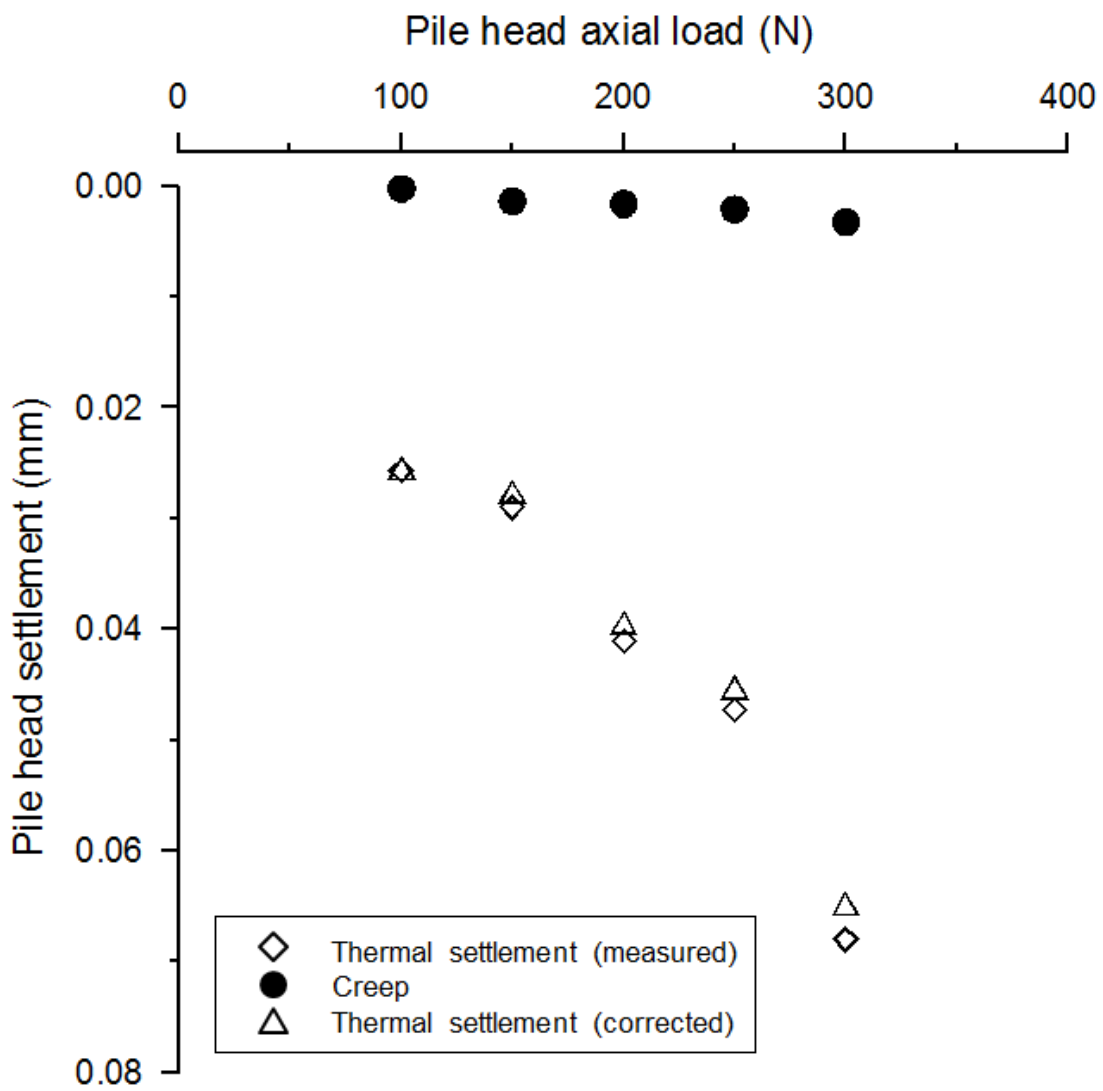


Figure 11. Results of tests F3-F7 for the thermal phase - Pile head settlement versus pile head axial load